Appl. Phys. B (2013) 112:279–283
DOI 10.1007/s00340-013-5431-4

Applied Physics B
Lasers and Optics

Pump power dependence of the spatial gating properties of femtosecond optical Kerr effect measurements

Xiaofang Wang · Pengchao He · Lihe Yan · Jinhai Si · Feng Chen · Xun Hou

Received: 25 October 2012 / Accepted: 21 March 2013 / Published online: 30 March 2013

Abstract The pump power dependence of the spatial gating properties of femtosecond optical Kerr gate (OKG) was investigated using coaxial two-color optical Kerr measurements in CS_2. As the pump power increased, the spatial pattern of the optical Kerr signals changed from a Gaussian spot to a ring form, and then a spot surrounded by a concentric ring, successively. By comparing the experimental data with the calculation results and measuring the pump power dependence of the OKG signal intensity, we demonstrated that the spatial variation of OKG transmittance could be attributed to the non-uniform spatially distributed phase change of the probe beam, due to the transient birefringence effect induced by pump beam with transverse mode of a Gaussian distribution.

1 Introduction

For the past few decades, femtosecond optical Kerr gating (OKG) technique has been developed as a key tool to measure the nonlinear response of all kinds of materials [1–4]. This technique could provide an ultrafast measurement of broad wavelength range, ultrafast switching time, and high precision. Hence, it has been widely used in ultrafast imaging and microscopy areas, such as ballistic optical imaging [5–8], simultaneous three-dimensional (3-D) imaging [9–11], etc. Recently, this method has been successfully used to investigate the laser-produced plasma dynamics and propagation dynamics of laser pulses in a medium [12, 13].

In the OKG measurements, an intense linearly polarized pump beam passing through the nonlinear material will cause the refractive index change of the sample. When the probe pulse overlaps with the pump beam temporally, a phase shift occurs between the probe field components polarized parallel and perpendicular to the polarization plane of the pump pulse. The OKG signal intensity is given by [14, 15]:

$$I_{\mathrm{OKG}} = I_{\mathrm{probe}} \sin^2(2\theta) \sin^2(\Delta\phi/2). \quad (1)$$

Here, I_{probe} is the probe intensity. θ is the polarization angle between the pump and probe beams, which is fixed at 45° to optimize the OKG signal. And $\Delta\phi$ indicates the phase shift caused by the light-induced birefringence effect, which is proportional to the pump intensity.

In the previous reports, the OKG signals were considered quadratic dependening on pump power for the small phase shift [14–16]. In the OKG measurements, however, when a pump beam with a nonuniform intensity distribution, such as a Gaussian mode was used, it might induce spatially nonuniform distribution of the phase change of the probe beam. If the pump is of high intensity, the transmittance of the OKG setup might vary sinusoidally as a function of pump power, and the OKG signals would present different spatial profiles depending on the pump intensity distribution. Hence, it is important to research on the spatial gating property of the OKG setup, especially when it is used in ultrafast imaging and microscopy areas.

In this paper, we investigated the evolution of spatial profiles of the femtosecond OKG signals as a function of pump power in CS_2. With the increase of pump power, the spatial pattern of the OKG signals changed from a Gaussian spot to a ring form, and then a spot surrounded by

X. Wang · P. He · L. Yan (✉) · J. Si · F. Chen · X. Hou
Key Laboratory for Physical Electronics and Devices of the Ministry of Education and Shaanxi Key Lab of Information Photonic Technique, School of Electronic and Information Engineering, Xi'an Jiaotong University, Xianning-xilu 28, Xi'an 710049, China
e-mail: liheyan@mail.xjtu.edu.cn

a concentric ring, successively. Furthermore, the OKG signal intensity at fixed position showed different pump power dependence with the spatially integrated OKG signal intensity. A series of numerical analysis was performed to explain the experimental results. Both the experimental and numerical results indicated that the spatial variation of OKG transmittance was attributed to the non-uniform spatially distributed refractive index change induced by pump beam with transverse mode of a Gaussian distribution.

2 Experimental methods

Figure 1 illustrates the experimental setup. The experiment was performed using 65 fs, 800 nm pulses from a regeneratively amplified Ti: sapphire laser system (Libra-USP-HE, Coherent Inc.) operating at 1 kHz repetition rate. The laser beam with a Gaussian intensity profile was split into two. The first one passing through a time-delay device was used as the pump beam. The other one which was frequency doubled to 400 nm by a β-barium borate (BBO) crystal was used as the probe beam. The two beams were combined together by an unpolarized dichroic mirror (DM, with high reflective coating at 800 nm on one side and antireflective coating at 400 nm on the other side). Both of them were focused by a plano–convex lens (L3) with a focal length of 20 cm. A 2-mm thick quartz cell filled with CS_2 was placed 5 mm behind the focal point of the 800-nm pump beam. The pump beam radius in the sample was determined to be 190 μm at $1/e^2$, and the probe beam radius was enlarged about five times by the collimating lens (L2) behind BBO crystal, so that the probe intensity could be considered uniformly distributed compared with the pump. To avoid the white-light continuum generation, the pump energy was kept below 12 mW (about 0.01 J/cm^2) [17]. A polarizer in a cross-Nicol configuration was placed behind the Kerr medium. To optimize the OKG signal intensity, the temporal overlap was maximized at zero time-delay, and the polarization plane of the pump pulse was rotated by 45° with respect to that of the probe pulse using a half-wave plate. The probe fluence distribution after the polarizer was recorded by a CCD camera with a 4f system. To block the 800-nm pump light, a bandpass filter centered at 400 nm was used in front of the CCD camera.

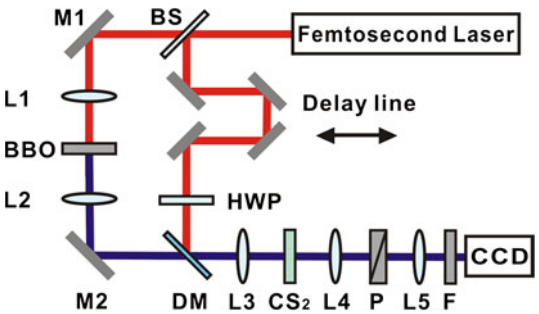

Fig. 1 Scheme of the experimental setup. *BS* beam splitter, *DM* dichroic mirror, *HWP* half-wave plate, *P* polarizer, *F* bandpass filter

3 Results and discussion

In our work, 31 image data of the OKG signal profiles were collected with the pump power varying from 1.85 to

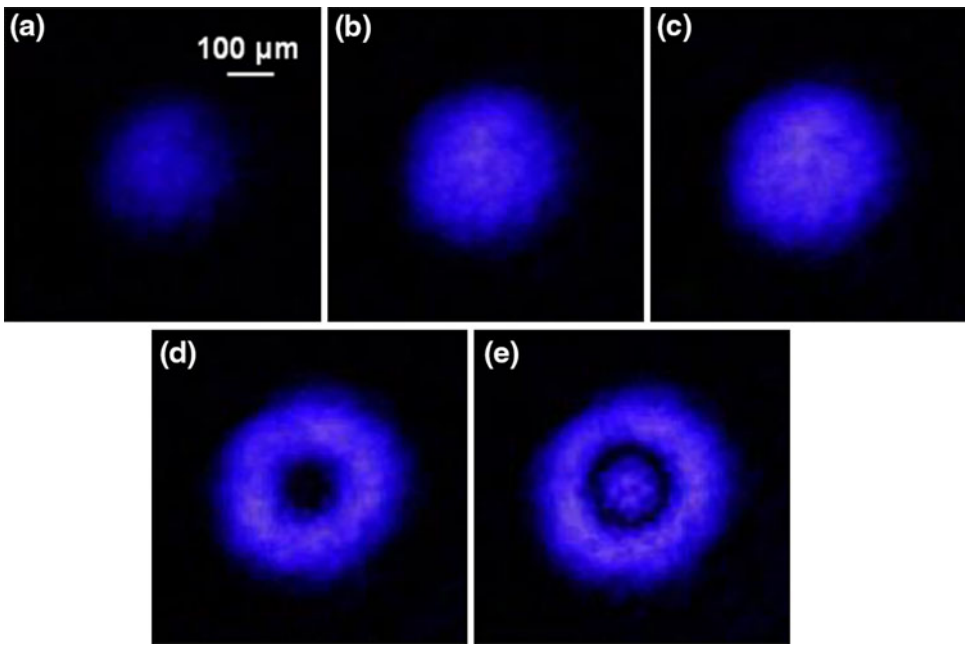

Fig. 2 OKG signal profile when the pump fluence was fixed at **a** 1.63 mJ/cm^2, **b** 3.39 mJ/cm^2, **c** 4.53 mJ/cm^2, **d** 8.53 mJ/cm^2, and **e** 10.46 mJ/cm^2, respectively

11.86 mW, and the corresponding pump fluence varying from 1.63 to 10.46 mJ/cm^2. Figure 2a–e shows five typical recorded probe patterns of these OKG signals when the pump fluence was adjusted to 1.63, 3.39, 4.53, 8.53, and 10.46 mJ/cm^2, respectively. The color scales in all the pictures were adjusted to the same range. When the pump fluence was relatively low (Fig. 2a–c), the total intensity of the OKG signal grew with the increase of the pump fluence, and the pattern of each signal was a spot with Gaussian distribution. As the pump fluence increases higher, however, the OKG signal pattern changed to a ring form and then a spot surrounded by a concentric ring, as shown by Fig. 2d, e, respectively.

In our experiments, the pump beam with a Gaussian intensity distribution can be expressed by

$$I_{\text{pump}}(r) \propto F_{\text{pump}} \mathrm{e}^{-2r^2/r_0^2}. \quad (2)$$

Here, F_{pump} is the pump fluence, and r_0 is the radius of the Gaussian beam, which has been determined to be 190 μm. As the polarization angle between pump and probe beams, θ, is set at 45°, the spatial intensity of probe light with an uniform distribution passing through the polarizer behind the Kerr medium can be written as

$$I_{\text{OKG}}(r) = A \sin^2\left(BF_{\text{pump}} \mathrm{e}^{-2r^2/r_0^2}\right). \quad (3)$$

Here, the term in the bracket denotes the phase shift $\Delta\phi(r)/2$ caused by birefringence effect. A and B are constants. The OKG signal intensity, $I_{\text{OKG}}(r)$, reaches the peak value of A when the phase shift $\Delta\phi(r)/2 = n\pi/2 (n = 1, 3, 5, \ldots)$ and reduces to the valley value of zero when $\Delta\phi(r)/2 = n\pi (n = 0, 1, 2, \ldots)$. Since the laser transverse mode is of a Gaussian distribution, the phase shift of the probe, which is proportional to the pump intensity, decreases along the radial direction. Consequently, the transmittance of the OKG setup might present a spatially modulated intensity distribution when the pump fluence is increased.

To present the evolution of the OKG profiles more clearly, we acquired the one-dimensional exposure data along the horizontal radial direction from the collected images. The results corresponding to Fig. 2 are shown by the discrete solid points in Fig. 3a–d. When the pump fluence was adjusted to 1.63 and 3.39 mJ/cm^2, the maximum value of phase shift $\Delta\phi(r = 0)/2$ was smaller than π/2, and the OKG signals intensities were of Gaussian distribution as shown by Fig. 3a. And the brightness of the OKG profiles was shown by Fig. 2a–b. With increasing pump fluence, the phase shift might be close to π/2 around $r = 0$, and the OKG signals showed a top-flat profile as shown by Fig. 3b. In Fig. 3c, when the pump fluence was increased to 8.53 mJ/cm^2, the phase shift $\Delta\phi(r)/2$ increased to about π around $r = 0$, and decreased to π/2 at $r \approx \pm 120$ μm. Hence, the transmittance of the OKG setup presented a peak–valley–peak profile, and the OKG signal pattern showed a ring form as shown by Fig. 2d. As the pump fluence increased to 10.46 mJ/cm^2, the probe pulse experiences phase shift $\Delta\phi(r)/2$ as large as π/2 at $r \approx \pm 120$ μm and π at $r \approx \pm 60$ μm, while reaching to larger than π at around $r = 0$. Therefore, the OKG pattern presented a central spot surrounded by a concentric ring, and the one-dimensional OKG signal distribution presented

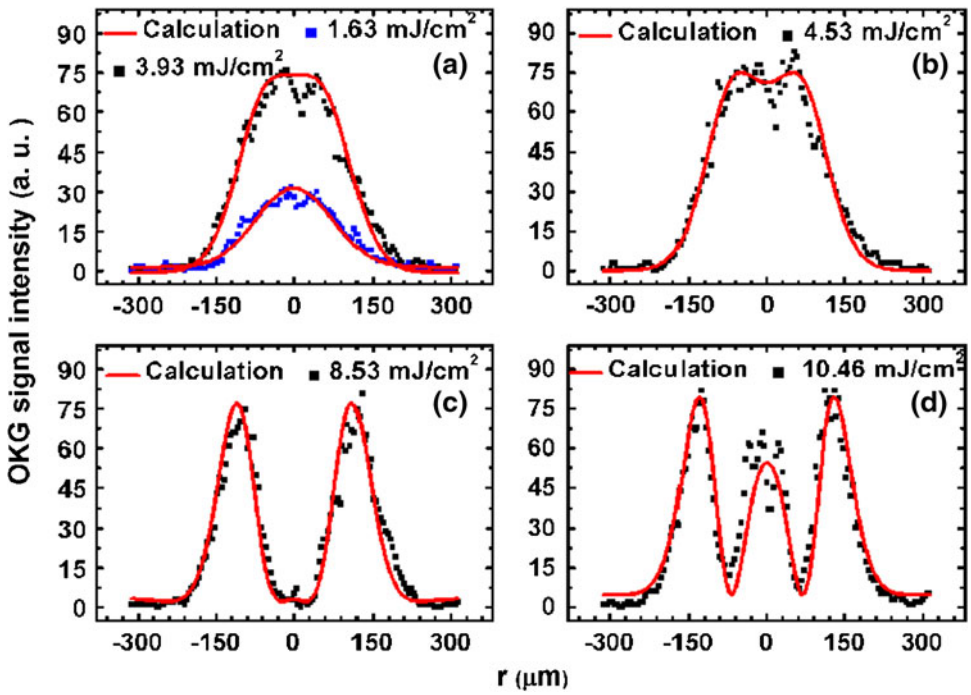

Fig. 3 One-dimensional OKG signal intensity distributions when the pump fluence was fixed at **a** 1.63 mJ/cm^2, **b** 3.39 mJ/cm^2, **c** 4.53 mJ/cm^2, **d** 8.53 mJ/cm^2, and **e** 10.46 mJ/cm^2, respectively. The *discrete solid points* are experimental results. The *red solid lines* indicate the calculated curves

a multi-peak profile, as shown by Figs. 2e and 3d, respectively.

Using Eq. (3), we fitted the one-dimensional OKG signal intensity distributions at different pump fluence, and the parameters A, and B in Eq. (3) were calculated to be 75.00 and 0.394 cm^2/mJ, respectively. The red solid lines in Fig. 3 indicate the calculated curves using Eq. (3) and the parameters obtained above. They accorded well with the experimental results as shown by the solid points, indicating that the spatial variation of the OKG transmittance was attributed to the transient non-uniform birefringence induced by pump beam with a Gaussian distribution.

The squares in Fig. 4a show the pump fluence dependence of OKG signal intensity at the fixed position of $r = 0$. The red solid line in the figure indicates the calculated results using Eq. (3), which can be simplified to a sinusoidal function of the pump fluence when the value of r is fixed. The squares in Fig. 4b indicate the spatially integrated intensity of the OKG signal profiles as a function of the pump fluence. By integrating Eq. (3), the spatially integrated OKG signal intensity can be expressed by

$$\int I_{\mathrm{OKS}}(r)\mathrm{d}s = \int_0^{+\infty} A\sin^2\left[BF_{\mathrm{pump}}e^{-2r^2/r_0^2}\right]2\pi r\mathrm{d}r. \qquad (4)$$

The red solid line with circles in Fig. 4b shows the calculated results using Eq. (4). Both the experimental results shown in Fig. 4a and 4b accorded well with the calculated results. The integrated OKG signal intensity, however, showed different pump fluence dependence with OKG signal intensity at the fixed position. It increased sharply at low pump fluence and then slowly when the pump fluence increased to be larger than 6 mJ/cm^2. This difference could be attributed to the spatial variation of the OKG profiles due to the nonuniform spatially distributed phase change induced by the pump beam.

In addition, we measured the dependence of the OKG signal intensity on the polarization angle between the pump and probe beams to better understand the origin of the OKG signals. The squares and triangles in Fig. 5 show the polarization dependence of the integral OKG signals, when the pump fluence fixed at 3.22 and 10.30 mJ/cm^2, respectively. In the experiments, we found the spatial patterns of the OKG signals remained the same at any polarization angle under the fixed pump fluence. So the phase shift of the probe is independent of the polarization angle. The solid line in Fig. 5 shows the theoretical curve of the polarization dependence of the OKG signals using Eq. (2). The polarization dependence of the OKG signals showed a period of $\pi/2$, with the maximum and minimum values occurring at $n\pi/2 + \pi/4$ and $n\pi/2 (n = 0, 1, 2, \ldots)$, respectively. Hence, the OKG signals could be attributed to light-induced birefringence effect.

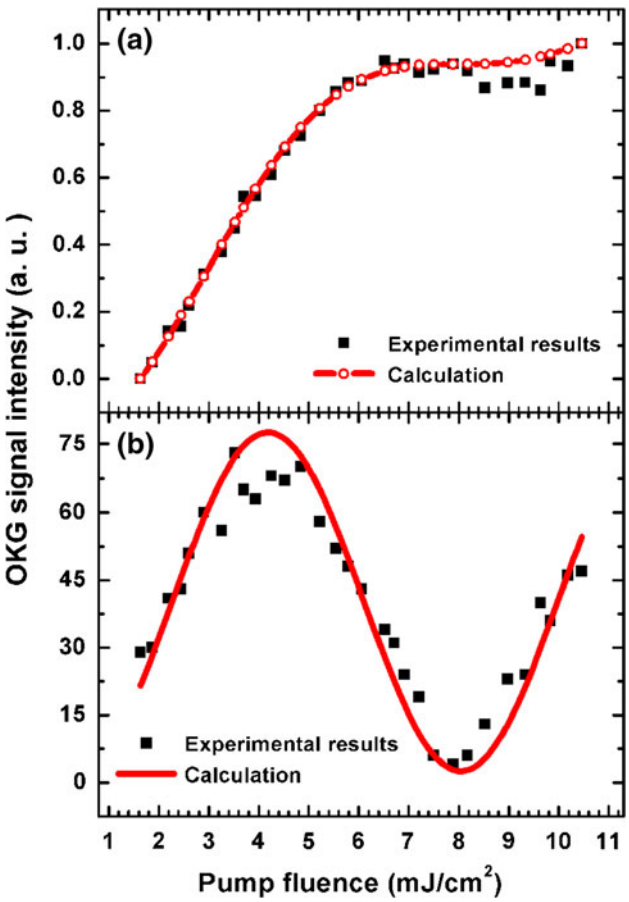

Fig. 4 Pump fluence dependence of **a** OKG signals at $r = 0$, and **b** spatially integrated exposure intensity of OKG signals. The *squares* are experimental results. The *red solid line* indicates the calculated curves

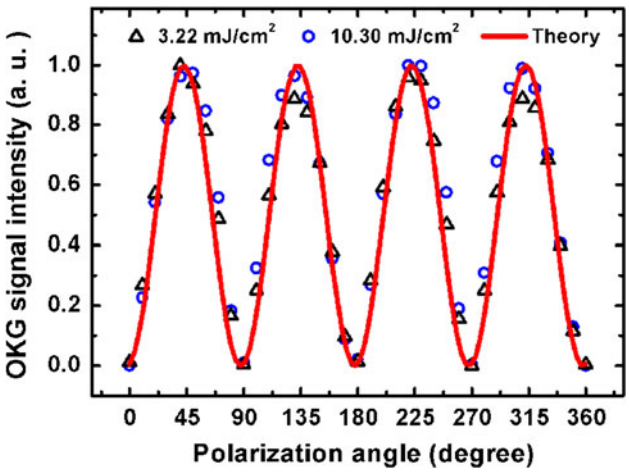

Fig. 5 Polarization dependence of OKG signals, when the pump fluence was adjusted to 3.22 and 10.30 mJ/cm^2, respectively. The *squares* and *triangles* are experimental results. The *red solid line* indicates the theoretical curve. The experimental results and the theoretical curve were both normalized to 1

Finally, the spectra of the OKG signals at different pump fluence were measured, which showed the same structure with that of the incident probe light. Because the response time of CS_2 lasted more than 1 ps, which was much slower than the probe pulse duration, the different wavelength components of the probe light experienced the uniform refractive index changes induced by the pump pulse. Hence, the spectral structure of the probe light passing through the OKG showed no obvious change.

4 Conclusions

In conclusion, we investigated the pump power dependence of the spatial gating properties of femtosecond optical Kerr effect measurements. When a pump beam with transverse mode of a Gaussian distribution was used in the femtosecond OKG measurements, it will cause a non-uniform spatially distributed refractive index change and the spatial variation of OKG transmittance. With increasing pump power, the OKG signal intensity distribution changed from a Gaussian spot to a ring form and then to a spot surrounded by a concentric ring, successively. Furthermore, the OKG signal intensity at fixed position showed different pump power dependence with the spatially integrated OKG signal intensity, due to the non-uniform distributed refractive index change induced by the pump beam with a Gaussian mode.

Acknowledgments This work was partially supported by the National Natural Science Foundation of China (NSFC) under the Grant No. 61235003, and the National Basic Research Program of China (973 Program) under Grant No. 2012CB921804. The authors also gratefully acknowledge the financial support provided by the NSFC under the Grant Nos. 61205129 and 11204236, as well as the Eyas Project supported by the Academy of Opto-Electronics, Chinese Academy of Sciences.

References

1. R. Righini, Science **262**, 1386 (1993)
2. Z. Yu, L. Gundlach, P. Piotrowiak, Opt. Lett. **36**, 2904 (2011)
3. J.Y. Lee, L. Yin, G.P. Agrawal, P.M. Fauchet, Opt. Express **18**, 11514 (2010)
4. K. Imakita, M. Ito, R. Naruiwa, M. Fujii, S. Hayashi, Appl. Phys. Lett. **101**, 041112 (2012)
5. L. Wang, P.P. Ho, C. Liu, G. Zhang, R.R. Alfano, Science **253**, 769 (1991)
6. R.R. Alfano, X. Liang, L. Wang, P.P. Ho, Science **264**, 1913 (1994)
7. M.A. Linne, M. Paciaroni, E. Berrocal, D. Sedarsky, Combust. Inst. **32**, 2147 (2009)
8. U. Bortolozzo, S. Residori, P. Sebbah, Phys. Rev. Lett. **106**, 103903 (2011)
9. K. Minoshima, T. Yagi, E. Abraham, H. Matsumoto, Opt. Eng. **38**, 1758 (1999)
10. A. Velten, T. Willwacher, O. Gupta, A. Veeraraghavan, M.G. Bawendi, R. Raskar, Nat. Commun. **3**, 745 (2012)
11. W. Tan, J. Tong, J. Si, Y. Yang, W. Yi, F. Chen, X. Hou, IEEE Photonic. Tech. L. **23**, 471 (2011)
12. D.R. Symes, U. Wegner, H.-C. Ahlswede, M.J.V. Streeter, P.L. Gallegos, E.J. Divall, R.A. Smith, P.P. Rajeev, D. Neely, Appl. Phys. Lett. **96**, 011109 (2010)
13. L.H. Yan, X.F. Wang, J.H. Si, S. Matsuo, T. Chen, W.J. Tan, F. Chen, X. Hou, Appl. Phys. Lett. **100**, 111107 (2012)
14. K. Dota, J.A. Dharmadhikari, D. Mathur, A.K. Dharmadhikari, Appl. Phys. B **107**, 703 (2012)
15. B. Schmidt, S. Laimgruber, W. Zinth, P. Gilch, Appl. Phys. B **76**, 809 (2003)
16. L.H. Yan, J.J. Yue, J.H. Si, X. Hou, Opt. Express **16**, 12069 (2008)
17. A. Brodeur, S.L. Chin, J. Opt. Soc. Am. B **16**, 637 (1999)